Doctor of Philosophy

The Biomechanical analysis of arm swing during gait in the elbow stiffness

The Graduate School
Of the University of Ulsan
Department of Medicine
Jae-Man Kwak

The Biomechanical analysis of arm swing during gait in the elbow stiffness

Supervisor: In-Ho Jeon, M.D., Ph.D.

A Dissertation

Submitted to
the Graduate School of University of Ulsan
In partial Fulfillment of the Requirements
for the Degree of

Doctor of Philosophy

by

Jae-Man Kwak

Department of Medicine
Ulsan, Korea
August 2021

The Biomechanical analysis of arm swing during gait in the elbow stiffness

This certifies that the dissertation of Jae-Man Kwak
is approved.

Committee chairman: Kwang Won Lee, MD, PhD

Committee member: Seung Jun Hwang, MD, PhD

Committee member: Gu-Hee Jung, MD, PhD

Committee member: Kyoung Hwan Koh, MD, PhD

Committee member: In-Ho Jeon, MD, PhD

Department of Medicine
Ulsan, Korea
May 2021

TABLE OF CONTENTS

ACKNOWLEDGEMENT

First and foremost, praises and thanks to the good Lord for his showers of blessings throughout my years of study as well as in this research work until the completion of this Ph.D study.

It is my genuine pleasure to express my sincere gratitude to my adviser, Prof. Jeon In-Ho, for the endless support during my Ph.D study. His guidance has helped me at all times of my research and dissertation writing. This research work and dissertation would not have been possible without his dedication and keen interest above all his overwhelming attitude to encourage his students. I would also like to express special gratitude to Prof. Jung Gu-Hee from the Department of Orthopedic Surgery, Gyeongsang National University, for his endless support with sincere advice and guidance since my residency. Apart from my adviser, I would like to thank the rest of my thesis committee, Prof. Lee Gwang Won (Department of Orthopedic Surgery, Eulji University), Prof. Hwang Seung Jun (Department of Anatomy, Ulsan University), and Prof. Koh Kyoung-Hwan (Department of Orthopedic Surgery, Ulsan University) for the time spent during my thesis review and defense, insightful comments, and critics and challenging questions.

I owe a deep sense of gratitude to Prof. Shawn O'Driscoll from the Department of Orthopedic Surgery, Mayo Clinic, Rochester, MN, USA, for his countless teaching, guidance, and passionate sharing of values as an orthopedic surgeon and Christian during my research fellowship in Mayo Clinic. In addition, I would like to thank Prof. James S. Fitzsimmons from the Biomechanical Core Facility, Mayo Clinic, for supporting the biomechanical study during my stay at Mayo Clinic. I am also grateful for the support from my trustful colleagues, Dr. Erica Kholinne from Indonesia, Dr. Yucheng Sun from China, Dr. Dani Rotman from Israel, Dr. Jorge Rojas Lievano from Columbia, and Dr. Alhazmi M. Adel from Saudi Arabia, for the massive support and feedback during my research work.

Moreover, I am also grateful to a very good researcher, Mr. Kang Bokku from the Department of Mechanical Engineering, Kyungpook National University, for the gait analysis with motion tracking technology. I also would like to recognize the help from my laboratory researcher, Ms. Shin You Jin, Ms. Heo Yijin, Ms. Heo Eejung, and Mr. Lee Jonghoon.

May 2021

Author

Jae-Man Kwak

ABSTRACT

Background and purpose: The arm swing plays a role in gait by assisting the forward movement with the maintenance of the trunk balance. This study evaluates the biomechanical characteristics of the shoulder and elbow and their alteration in elbow stiffness.

Materials and methods: The study included (1) biomechanical analysis and (2) computational musculoskeletal modeling based on motion tracking. This biomechanical study included eight fresh frozen specimens from individuals of both genders. Analysis was performed using Tekscan, and biomechanical analysis was performed with a custom-designed jig system with gravity-assisted muscle contracture. Fifteen participants without musculoskeletal or gait disorders were included for computational modeling. Three-dimensional (3D) motion tracking system using three Azure Kinect was used to obtain information for the 3D location of each joint. Computational modeling using The AnyBody Modeling System was performed to calculate the joint moment and range of motion during the arm swing of the gait.

Results: In biomechanical study, stage 2 contact pressure was significantly increased compared with stage 0 (mean contact pressure in the resting position, $P<0.0001$; mean contact pressure in the passive swing, $P=0.039$; peak contact pressure in the passive swing, $P<0.007$). In the computational modeling results, the elbow range of motion (ROM) of flexion–extension in stages 1 and 2 was significantly increased compared with stage 0 in the nondominant arm as the control group (stage 0 vs 1, $P<0.001$; stage 0 vs 2, $P=0.008$). Shoulder ROM of flexion–extension in stage 2 was significantly increased compared with stage 0 (stage 0 vs 2 in dominant, $P<0.001$; stage 0 vs stage 2 in nondominant, $P<0.001$).

The joint moment of the elbow in flexion–extension was significantly increased in stages 1 and 2 compared with stage 0 in the dominant arm (stage 0 vs 1, P=0.029; stage 0 vs 2, P<0.001) and in the nondominant arm (stage 0 vs 1, P=0.001; stage 0 vs 2, P<0.001). The joint moment of shoulder in flexion–extension in stage 2 was significantly increased compared with stage 0 in the dominant (stage 0 vs 1, P=0.569; stage 0 vs 2, P=0.005) and nondominant (stage 0 vs 1, P=0.039; stage 0 vs 2, P=0.015) arms.

Conclusions: The elbow bears the load created by gravity and muscle contracture in the resting and dynamic arm swing movement. Elbow joint stiffness increases the load-bearing in the resting position and the dynamic arm swing motion. The ipsilateral and contralateral shoulder joint seems to compensate for the decreased elbow motion by increasing the ROM of the shoulder joint. Therefore, the moment of both shoulder joints was also increased.

Clinical relevance: The current study showed that elbow stiffness should be managed not only for pain relief and limited motion but also to delay the arthritic process.

Keywords: arm swing, gait, elbow, shoulder, joint reaction force, contact pressure, biomechanics, cadaveric, motion tracking, computational musculoskeletal modeling.

LIST OF FIGURES

LIST OF GRAPHS

LIST OF TABLES

INTRODUCTION

1. Background

1.1.1 The elbow as a weight-bearing joint

The upper limbs are free from the role of weight-bearing because humans walk with two legs. The assertion that the elbow is not a weight-bearing joint has been commonly accepted as a traditional understanding of the human joint compared with the tetrapod joint. However, it does not mean that the elbow joint is completely free from loadbearing. Although precisely determining joint contact loads generated across the elbow is not simple, the elbow has been discovered to bear force in a variety of activities. The resultant forces generated at the ulnohumeral joint have been shown to reach one-half times the body weight during normal daily activities.[1] Chadwick and Nicol used sophisticated three-dimensional mathematical modeling, dynamic grip strength measurements, and video kinematic analysis and reported that resultant forces of up to two times bodyweight could occur across the ulnohumeral joint during motions commonly seen in occupational duties (e.g., lifting, moving, and placing 2-kg weights). Forces of up to three times body weight have been calculated to occur across both the ulnohumeral and the radiocapitellar joint during strenuous lifting. Dynamic loading, as seen during throwing or heavy pounding, produces forces of more than six times the body weight.[2-4] Individuals who perform manual labor or require wheelchair or crutch assistance may therefore be expected to produce large loads across the elbow on a more regular basis.[5] Although extreme loads are not likely to be experienced as frequently in the elbow as in the lower extremity joints during walking, the total articular surface of the elbow is also extremely small compared with that of the hip or knee. The elbow should also face the variable force in daily activity or sports due to the shoulder joint (e.g., throwing, swing, pushing, and pulling). However, no biomechanical study was evaluated to discover load-bearing in daily activity.

1.1.2 Arm swing in a gait

Humans walk bipedally, and the reason why humans normally swing arms during gait is unclear because this has no direct propulsion function. Historically, the models used in gait studies have often

been simplified to exclude the arms by modeling the head (H), arms (A), and trunk (T) into a HAT unit assuming that this unit moves as one mass.[6, 7] However, studies on gait for decades also included the analysis of the arm swing during gait because walking has been discovered to require the coordination of the whole body. A significant coordinated movement exists in the head, trunk, and pelvis orientation related to walking speed and pattern. Meyns et al. reviewed the literature and concluded that arm swing during human gait reduces energetic cost by as much as 8%, and converging evidence was noted that swinging the arms during gait facilitates leg movements.[7] In addition, arm swing during gait is not passive but driven by muscle activity that was confirmed by electromyographic findings.[8] However, how the arm swing exactly works (i.e., generated by accelerations at the shoulder girdle, inertia, and gravity) seems to still be an ongoing study. Clinical research showed that the asymmetry of arm swing has been proposed as a parameter for early-stage Parkinson's disease.[9, 10] However, no studies for gait analysis in the pathologic condition of the upper limb have been presented.

1.1.3 The elbow stiffness

The elbow joint is particularly prone to stiffness due to its anatomical and biomechanical complexities. The elbow has two degrees of freedom that were allowed by two joints (ulnohumeral and radiocapitellar joint), and the available movements in space are flexion, extension, pronation, and supination. Morrey et al. defined the arc of movement of the functional elbow during the daily activity of 100°, both for flexion–extension (30°–130°) and for pronation–supination (50° pronation and 50° supination).[11] Based on the definition of the functional range of motion (ROM), elbow stiffness is defined as the loss of movement >30° in extension and loss of flexion <120°.[12] Stiffness is one of the common pathologic conditions that required surgical release to recover the functional ROM for daily activity. In addition, elbow stiffness interferes with the primary activities of daily life (e.g., personal hygiene, eating, and dressing).[13] One of the causes of elbow stiffness is the consequence of the degenerative condition with marginal osteophyte and traumatic sequelae. No biomechanical research for elbow stiffness was reported although several studies have been done to understand the etiology, causes, management, and surgical technique. The main obstacle for the issue is that the stiff model of

the elbow is not introduced and validated with the cadaver. The modeling using the cadaver have lots of barriers to implement the pathologies because the causes of the stiff elbow and target pathologies are not single but multicomponent (e.g., loose bodies, osteophyte, capsule and muscle or tendon contracture). The modeling for stiffness due to the posterior osteophyte only in the present biomechanical study, which blocks the olecranon and extension, was limited and consequently created and suggested.

2. Research goal and null hypothesis

Research goal

1. The understanding of the biomechanical characteristic or change in the stiff elbow in the resting (or neutral) position of the arm using the cadaveric model.
2. The understanding of the biomechanical characteristic or change in the stiff elbow in the arm swing of a gait using computational musculoskeletal modeling based on motion tracking.

Null hypotheses

The null hypotheses included:

1. No difference exists in the articular contact pressure of the elbow by comparing the *nonstiff* and *stiff models* in in vivo study.
2. The degree of stiffness would not affect the increase of the joint loading of the elbow.
3. No difference of joint moment of the elbow and shoulder was noted by comparing *nonstiff* and *stiff models* in the arm swing of a gait.

MATERIALS AND METHODS

All data, unless otherwise stated, are presented as means±standard deviation. Biomechanical testing and data collection were carried out using a previously established model as described below.[14-17]

1. Biomechanical study

1.1. Specimen preparation

Eight fresh frozen cadaveric unpaired upper limbs (five right and three left), from the fingertip to the midhumerus, were thawed at room temperature overnight. The average age of the cadaver was 58–72 years old. All the cadavers have been screened for a previous history of upper limb pathology including trauma and contractures. The pre-experimental examination for the ROM measurement and varus, valgus, and rotational stability was conducted. None of the specimens had a flexion contracture of >10°, a pronation–supination rotation arc <140°, or radiologic evidence of arthritis or deformity. Any specimen with cartilage erosion to the subchondral bone was excluded, but specimens exhibiting shallow erosion with fibrillation and fissuring with normal joint contact were not discarded. Any specimen with ligament insufficiency (detected either by performing the posterolateral rotatory drawer test or after direct visualization of the ligaments) was excluded.[18] The skin and subcutaneous fat were removed from the midhumerus to 5 cm distal to the elbow joint. The biceps, brachialis, and triceps muscle bellies were removed while their tendon insertions were preserved and prepared with locking Krackow stitches using a 36–kg (80 lb) test braided Dacron fishing line. The humeral origins of the flexor–pronator and the extensor–supinator muscles were preserved. The anterior capsule was excised, with care taken not to injure the collateral or annular ligaments, to permit placement of the pressure transducer. Parallel holes were made in the proximal humeral end of the specimen to fix the custom-made zig system. A medial column humeral osteotomy was made, and a 2-mm groove was created in the bare area of the olecranon for sitting of the sensor on the olecranon (Figure 1). A Tekscan 4205 thin-film pressure transducer (Tekscan, South Boston, MA, USA) was inserted from the anterior to the posterior after anterior capsule excision until the end of the sensor reached the olecranon bare area groove and covered both the ulnohumeral articulations.

The medial column osteotomy was fixed with three or four screws and washers (one Arbeitsgemeinschaft für Osteosynthesefragen [AO] 3.5-mm cancellous screw for intercondylar fixation and two or three AO 3.5-mm cortical screws for distal humerus fixation).

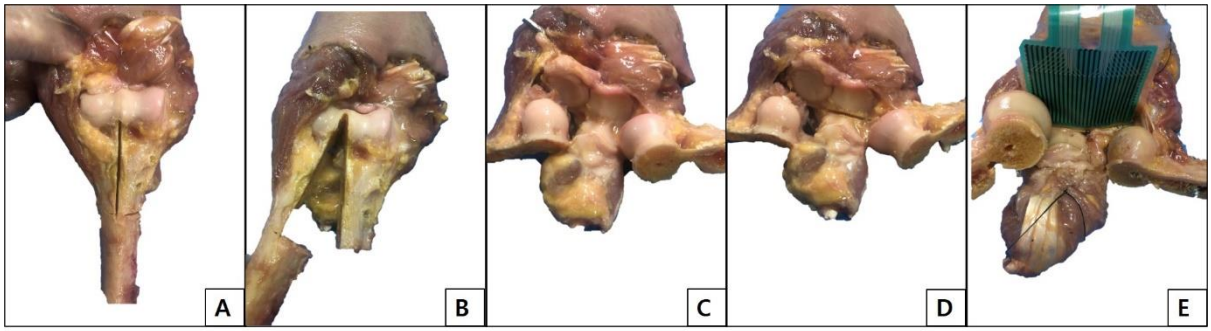

Figure 1. Specimen preparation for sensor placement. The anterior capsule was excised, with care taken not to injure the collateral or annular ligaments, to permit placement of the pressure transducer. A medial column humeral osteotomy was made and a 2-mm groove was created in the bare area of the olecranon for sitting of the sensor on the olecranon. The sensor was inserted from the anterior to the posterior after anterior capsule excision until the end of the sensor reached the olecranon bare area groove and covered both the ulnohumeral articulations.

1.2. Pressure transducer preparation

The 4205 sensors were preconditioned and calibrated following the manufacturer's recommendations.[14] A Tekscan 4205 thin-film pressure transducer (Tekscan) with a saturation pressure of 8.3 MPa (84.4 kg/cm^2) was prepared and inserted into the joint from the anterior to the posterior as previously reported.[15] The osteotomized medial humeral condyle was fixed with four screws as previously, and the sensor was secured in place by tying it to two proximal screws in the proximal posterior aspect of the ulna. The thin-film Tekscan sensor has been validated for measuring pressure in rounded contact areas[19] and has been used in earlier reports of joint contact pressures,[20, 21] specifically including use within the elbow.[14-17, 22] Each 4205 sensor has one 45.7-mm × 41.9-mm matrix, consisting of 528 sensels (individual detection units of pressure) located on the conductive ink grids. The 4205 sensors were preconditioned and calibrated following the manufacturer's recommendations. To reduce the friction between the joint surface and the sensor, 2 mL of mineral oil

(Sigma-Aldrich, St. Louis, MO, USA) was applied to the joint after sensor insertion. The articular surfaces and the tendons were frequently moistened with normal saline during testing.

1.3. Specimen mounting

Specimens were mounted in a custom-made apparatus to mimic the neutral position of the arm with the shoulder in 0° of the forward flexion and 0° of rotation (Figure 2A). The forearm was placed in neutral. The biceps, brachialis, and triceps were connected to the weight (2.5 kg, biceps and brachialis; 5 kg, triceps) to simulate muscle loads intended to provide dynamic joint stability. Force was applied in a 1:1:2 ratio with the brachialis, biceps, and triceps receiving 24.5, 24.5, and 49 N, respectively.[14-17, 22] These values were selected after pilot study tests were performed evaluating different loads.

The distance of each pulley from the joint line and humeral axis was set to simulate the physiologic position of the tendons 5.5 cm proximal to the joint line. The brachialis, biceps, and triceps pulleys were set at 2, 3.5, and 2 cm away from the humeral axis, respectively. The elbow was passively flexed by pulling a braided 36-kg test polyester line perpendicular to the forearm over the ROM to avoid application of stabilizing or distracting forces created by direct manual manipulation of the forearm.[14-17, 22]

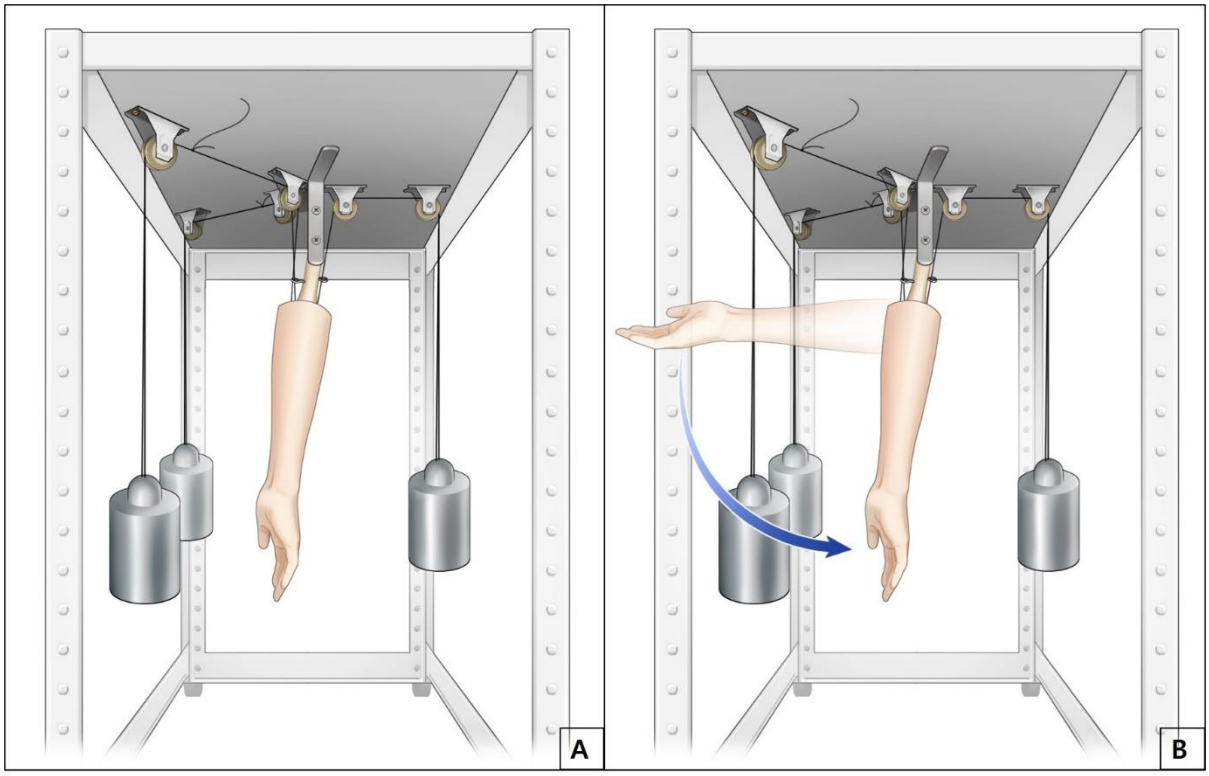

Figure 2. Custom-made zig system. A Specimens were mounted in a custom-made apparatus to mimic the neutral position of the arm with the shoulder in 0° of the forward flexion and 0° of the rotation. **B** The passive swing was performed by dropping the forearm from 90° of the elbow flexion.

1.4. Testing protocol

The elbow was tested in two conditions (the resting and passive swing). Contact pressure was recorded for 3 s in the resting position that was in the neutral position of the humerus. The passive swing was performed by dropping the forearm from 90° of the elbow flexion (Figure 2B). The specimens were tested sequentially in three stages of stiffness (stage 0, no stiffness; stage 1, 30° of extension limitation; and stage 2, 60° of extension limitation). A stiff model was created in a sequential manner for each stage after data collection was completed in stage 0. The stiff model of the elbow was created by blocking the olecranon by inserting 2.0 K-wire into the olecranon fossa horizontally with the intercondylar axis (Figure 3A). With the placement of the elbow at the 30° of flexion, K-wire was inserted just above the tip of the olecranon so the K-wire block does not extend to the elbow further than 30° (stage 1, Figure 3B). After collecting data for stage 1, the second K-wire

was inserted after further flexion with 60° of flexion (stage 2, Figure 3C). The protocol was similarly repeated to collect data during the passive swing.

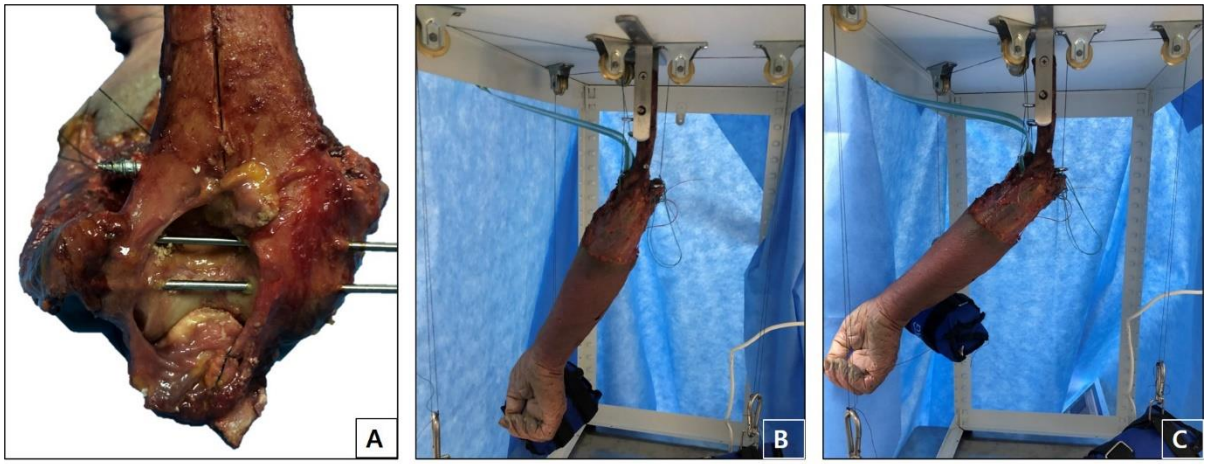

Figure 3. Cadaveric modeling for elbow stiffness The stiff model of the elbow was created by blocking the olecranon by inserting the 2.0 K-wire into the olecranon fossa horizontally with intercondylar axis (**A**). With the placement of the elbow at 30° of flexion, the K-wire was inserted just above the tip of the olecranon so the K-wire block does not extend to the elbow further than 30° (stage 1, **B**). After collecting data for stage 1, the second K-wire was inserted after further flexion with 60° of flexion (stage 2, **C**).

1.5. Data measurements

Data were recorded using the Tekscan software (I-Scan). The outline of the coronoid and radial head was registered using the Tekscan sensor and a blunt probe at the beginning of each set of tests (stages 0–2). The contact pressure was recorded for 3 s in the resting position. The mean contact (in kilopascal) and peak contact pressures were used for comparison among the two groups (stages 1–2) with the intact elbow (stage 0) in the swing motion. The peak contact pressure was separated and excluded to calculate the mean contact pressure in the swing motion. All Tekscan data were processed using a previously published technique.[15, 16]

2. Computational modeling based on the motion tracking data

2.1. Subjects

This study included motion tracking data collected from healthy participants of 15 individuals (eight females and seven males; mean age, 25±5 years) with no musculoskeletal or gait disorder. Mean height was 170.6±8.9 (cm) and mean weight (kg) was 65.8±12.1. All participants confirmed their hand dominance to be right. All subjects provided written informed consent before participating in the study.

2.2. Experimental setup for 3D motion capture

Figure 4. Experimental setup for motion tracking. The treadmill pointed directly toward the frontal depth sensor for the full-frontal plane view, and the others pointed to its side (*left arm*, *right arm*) orthogonally to the frontal camera centered in the treadmill.

Three markerless depth sensors (Azure Kinect; Microsoft, Redmond, WA, USA) as the motion tracking camera was placed on the flat ground. All depth sensors had zero-angle tilting and were mounted on three tripods. The treadmill was placed at the center of three cameras. The handrail of the

treadmill was removed to prevent occlusion to the cameras (Figure 4A). The distance (2 m) and height (1.5 m) of the cameras from the treadmill were fixed to ensure that the entire body was within the operating ranges of each sensor as suggested by the manufacturers.[23] The treadmill pointed directly toward the frontal depth sensor for the full-frontal-plane view and the others pointed to its side (left and right arm) orthogonally to the frontal camera centered in the treadmill (Figure 4B).

The motion during the experiment was captured at 30 Hz and data acquisition was proceed using the markerless motion capture software (iPi Motion Capture™, LLC, Moscow, Russia) based on the respective software development kits. Inverse dynamics were computed from the kinematic measurement (ROM, position, velocity, and acceleration of elbow and shoulder) value of the depth sensor data. Elbow was treated as 2 degree of freedom (DOF) joint, and its flexion/extension and pronation/supination angles were measured and moments were calculated for sagittal and axial planes, respectively. The shoulder joint was treated as a 3-DOF joint and its flexion/extension, abduction/adduction, and external rotation/internal rotation angle were measured and moments were calculated concerning sagittal, coronal, and axial planes, respectively. When the three depth sensors started body tracking, their monitoring PCs independently sent data to the main computer that collects data for synchronization.

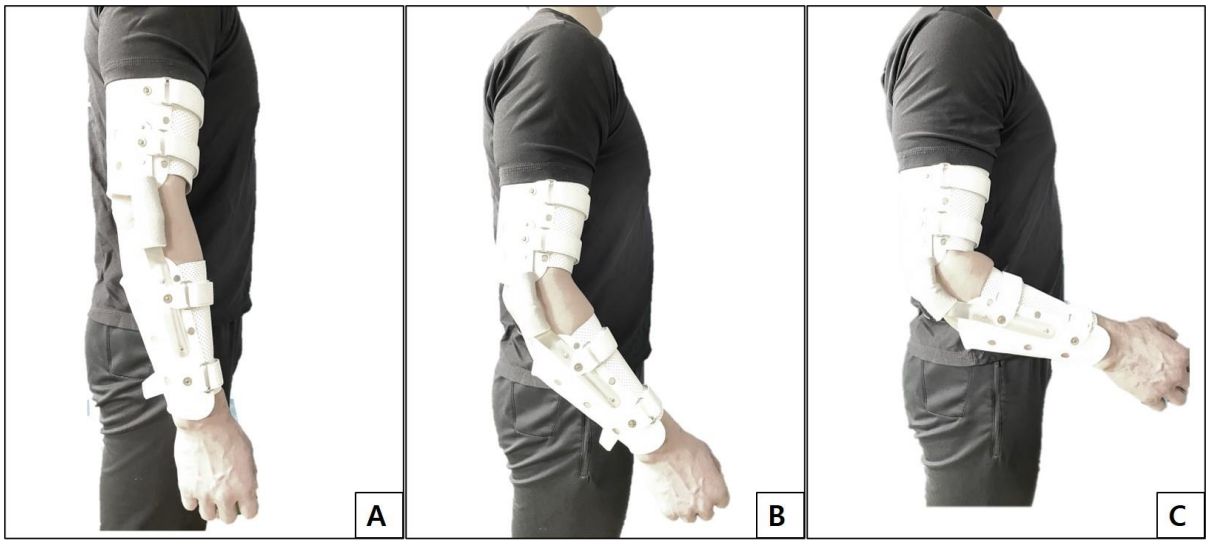

Figure 5. Stiff elbow modeling in vivo condition. The subjects wore the custom-designed elbow brace that allows setting the extension block at 0° (**A**), 45° (**B**), and 90° (**C**). The subjects were tested sequentially in four stages (normal, no brace; stage 0, brace with no extension blocking; stage 1, 45° extension blocking; and stage 2, 90° of extension blocking). After the recording was completed in the normal session, the subjects wearing the brace were tested sequentially for each stage (stages 0–2).

2.3. Experimental protocol

Subjects were instructed before the start of the experiment to warm up by walking at A constant speed controlled by the treadmill (walking, 1.11 m/s) for 60 s each to familiarize the apparatus. The constant speed for walking was selected based on a reference gait dataset for the 20–39-year-old age group.[24] Reference gait patterns of the speed (walking, 30 s per trial) were recorded by depth-censored cameras. The subjects wore the custom-designed elbow brace that allows setting the extension block at 0° (Figure 5A), 45° (Figure 5B), and 90° (Figure 5C). The subjects were tested sequentially in four stages (normal, no brace; stage 0, brace with no extension blocking; stage 1, 45° extension blocking; and stage 2, 90° of extension blocking). After the recording was completed in a normal session, the subjects wear the brace was tested in a sequential manner for each stage (stages 0–2).

2.4. Computational musculoskeletal modeling

The specific X-Y-Z locations obtained from the motion capture session were used as input to the musculoskeletal model in the AnyBody Modeling System™ software (AnyBody Technology, Aalborg, Denmark, version 7.3.0). A global axis specified the environmental factor of gravity (−9.81 m/s^2 in the superior–inferior direction). The upper body portion of the full-body model from the AnyBody™ Managed Model Repository (version 2.3.0) was used for both normal and braced conditions. The elbow brace worn by the participant during the braced condition weighed <300 g and was considered negligible for the force computations of the current study. The model is comprised of the pelvis, trunk, neck, and arms, each consisting of multiple bones. The arm consists of several joints including three spherical joints (sternoclavicular, acromioclavicular, and glenohumeral), three

revolute joints (elbow and two in the wrist), as well as pronation/supination of the forearm. The model also includes lumbar, thoracic, and cervical spines and contains multiple muscle fascicles that make up each muscle of the upper body. The generic model was scaled to each subject using anthropomorphic data. Muscle groups were sectioned into force vectors connected at two points in the body representing the origin and insertion points for the muscle. Model parameter identification and inverse dynamic analysis were conducted following previously validated study.[25]

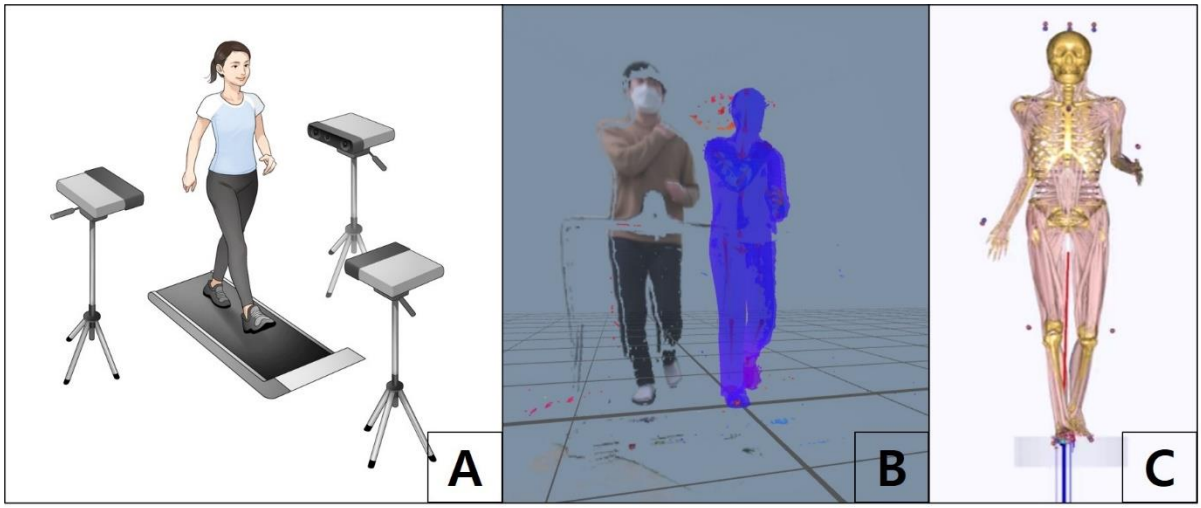

Figure 6. The process of inputting the location data for computational modeling. A Motion tracking and collecting the location data with three depth cameras. **B** The motion during the experiment was captured at 30 Hz, and data acquisition proceeded using the markerless motion capture software (iPi Motion Capture™, LLC). **C** The specific X-Y-Z locations obtained from the motion capture session was used as input to the musculoskeletal model in AnyBody Modeling System™ software (AnyBody Technology, version 7.3.0).

2.5. Data analysis

Data analysis was completed using MATLAB. The data were segmented into trials, where segmented gait patterns were normalized to the gait cycle. Only seven gaits in the middle of each 30-s recording were selected and averaged for data analysis. A gait was defined as duration that is from the point that a heel of the reference foot starts to touch the ground to the endpoint of the terminal swing of the reference foot (Figure 7B).

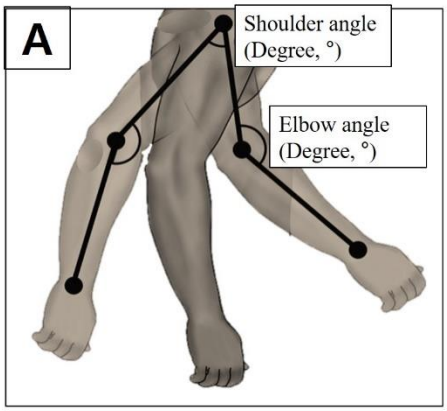

Normal data (n=15)	Dominant	Non-dominant
Elbow (angle, mean ± S.D.)		
Flexion-Extension	29.7±10.2	31.9±12.1
Pronation-Supination	14.2±3.2	14.8±2.7
Shoulder (angle, mean ± S.D.)		
Flexion-Extension	56.4±12.7	60.3±13.9
Rotation	25.6±5.2	23.3±6.7
Abduction-Adduction	19.4±5.4	18.8±7.5

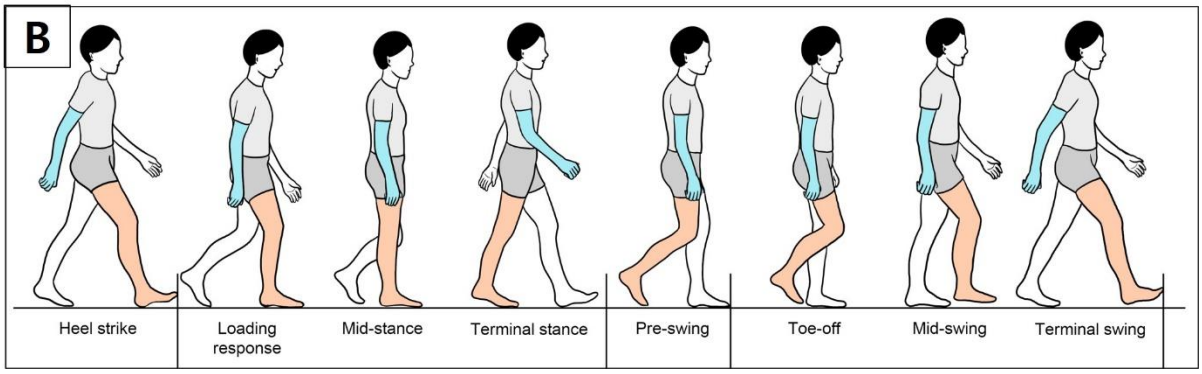

Figure 7. Normative data for arm swing in a gait. A gait was defined as the duration that is from the point that a heel of the reference foot starts to touch the ground to the endpoint of the terminal swing of the reference foot.

All postacquisition data processing was performed in Python 3.7.4. After the normalized kinematic gait patterns of the 10 sampled walking steps were averaged, the ROM in terms of maximum and minimum joint angles were computed for each walking trial. The mean joint moment of each time frame in each joint was calculated. All moment measurements are in Newton meter.

3. Statistical analysis

The statistical analysis was performed under the supervision of a biostatistician. The Kolmogorov–Smirnov test was used for normality distribution for all datasets. All descriptive and quantitative analyses were conducted using SPSS version 22.0 (SPSS, Inc, Chicago, IL, USA).

Each stage was analyzed using repeated-measures analysis of variance with least-squares post hoc comparisons where appropriate, with $P<0.05$ considered significant. In a biomechanical study, on the basis of power calculations derived from historical data,[15] this study determined an 80% chance of

detecting a significant difference in mean contact pressures between stages 0 and 2 of 50 kPa with $p<0.05$. In computational modeling analysis, the significance level was set at <0.05. The sample size of 15 for each group was estimated to achieve a 0.80 power detecting a significant difference in the mean joint moment of the elbow in flexion–extension between stages 0 and 2 of 10 Nm with $p<0.05$.

RESULTS

1. Biomechanical study

1.1. Contact pressure in resting position

In stages 0, 1, and 2, the mean contact pressures were 279±23, 302±6, and 349±23 kPa, respectively. Although the mean contact pressure in stage 1 was increased compared with that in stage 0, it did not achieve statistical significance (*P*=0.100). However, the increases of mean contact pressure in stages 2 versus 0 were significant (*P*<0.0001).

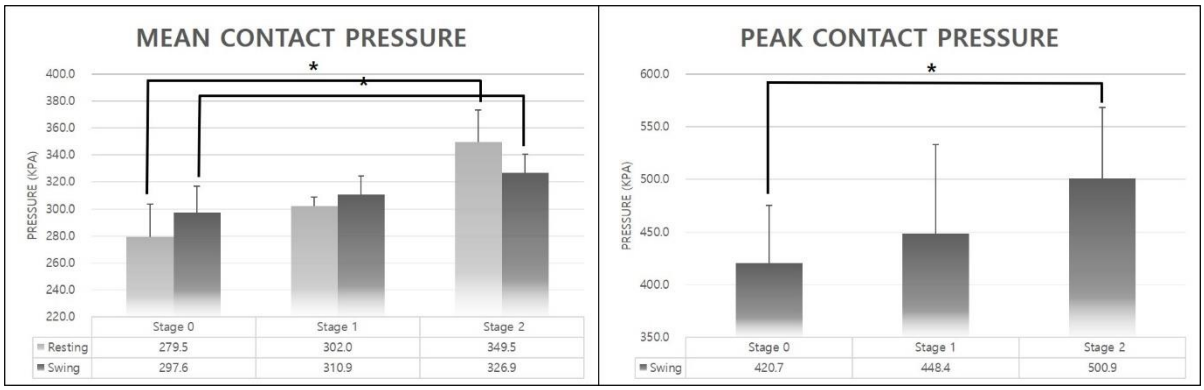

Graph 1. Mean and contact pressure in biomechanical study.

1.2. Contact pressure in the passive swing

The mean contact pressures were 297±19, 310±14, and 326±13 kPa in stages 0, 1, and 2, respectively. The mean contact pressure in stage 0 did not achieve statistical significance compared with stage 1 (*P*=0.442), and the increases in mean contact pressure in stage 2 versus 0 were significant (*P*=0.039). In stages 0, 1, and 2, the peak contact pressures were 420±54, 448±84, and 500±67 kPa, respectively. The mean contact pressure in stage 1 did not achieve statistical significance compared with that in stage 0 (*P*=0.513), the increases in peak contact pressure in stages 0 versus 2 were significant (*P*=0.007).

Table 1. Comparison between stages in the swing session (mean contact pressure, kPa)

Stage		Mean difference	SD	Sig.[a]	95% C.I.[a]	
					Lower bound	Upper bound
0	1	−13.286	7.987	0.442	−39.543	12.972
	2	−29.286*	8.394	0.039	−56.881	−1.690
1	0	13.286	7.987	0.442	−12.972	39.543
	2	−16.000	5.782	0.098	−35.007	3.007
2	0	29.286*	8.394	0.039	1.690	56.881
	1	16.000	5.782	0.098	−3.007	35.007

Repeated-measure ANOVA

*The mean difference is significant at the 0.05 level.

[a]Adjustment for multiple comparisons, Bonferroni.

Table 2. Comparison between stages in the swing session (peak contact pressure, kPa)

Stage		Mean difference	SD	Sig.[a]	95% C.I.[a]	
					Lower bound	Upper bound
0	1	−27.714	17.821	0.513	−86.302	30.873
	2	−80.143*	15.968	0.007*	−132.637	−27.649
1	0	27.714	17.821	0.513	−30.873	86.302
	2	−52.429*	14.563	0.034*	−100.305	−4.553
2	0	80.143*	15.968	0.007*	27.649	132.637
	1	52.429*	14.563	0.034*	4.553	100.305

Repeated-measure ANOVA

*The mean difference is significant at the 0.05 level.

[a]Adjustment for multiple comparisons, Bonferroni.

2. Computational musculoskeletal modeling

2.1. ROM during a gait

2.1.1. Elbow

The mean ROM of the dominant arm during a gait was 29.7±10.2 and 14.2±3.2 in flexion–extension and pronation–supination, respectively. No significant difference exists between the normal swing (without brace) and stage 0 (with the brace on the dominant arm (right arm) but a free ROM) in flexion–extension (P=0.343). A significant difference was noted between the normal swing and stage 0 in pronation and supination (P=0.001). In the dominant arm (right arm in all participants), the ROM of flexion–extension was significantly decreased because the brace consistently blocked the extension of 45° and 90° in stages 1 and 2, respectively. The ROM of pronation–supination was also significantly decreased in all comparison between stages (stage 0 vs 1, P=0.019; stage 0 vs 2, P< 0.001). In the nondominant arm (no brace, control group), the ROM of the flexion–extension of stages 1 and 2 was significantly increased compared with stage 0 (stage 0 vs 1, P<0.001; stage 0 vs 2, P=0.008). No significant difference was noted in all comparison for ROM of pronation–supination between stages (stage 0 vs 1, P=0.743; stage 0 vs 2, P=0.970).

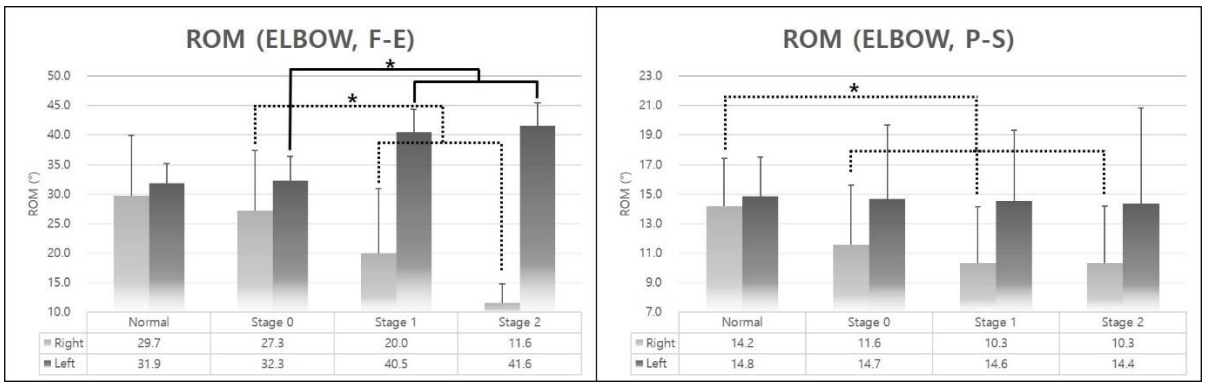

Graph 2. Elbow ROM inflexion–extension and pronation–supination.

2.1.2. Shoulder

The mean ROM of the dominant arm during a gait was 56.4±12.7, 25.6±5.2, and 19.8±4.6 in the flexion–extension, rotation, and abduction–adduction, respectively. No significant difference was noted between the normal swing (without brace) and stage 0 (flexion–extension, P = 1.000; rotation, P=1.000; abduction, P=1.000). In the dominant arm, the flexion–extension in stage 2 was significantly increased compared with stage 0 (stage 0 vs 1, P=0.115; stage 0 vs 2, P<0.001). No significant difference exists in all comparisons between stages in rotation (stage 0 vs 1, P=1.000; stage 0 vs 2, P=0.274) and abduction–adduction (stage 0 vs 1, P=0.870; stage 0 vs 2, P=1.000). In the nondominant arm (no brace, control group), the flexion–extension in stage 2 significantly increased compared with stage 0 (stage 0 vs 1, P=1.000; stage 0 vs 2, P<0.001). Rotation in stages 1 and 2 were significantly increased compared to stage 0 (stage 0 vs 1, P=0.008; stage 0 vs 2, P<0.001). No significant difference exists in all comparison between stages in the abduction–adduction (stage 0 vs 1, P=1.000; stage 0 vs 2, P =1.000).

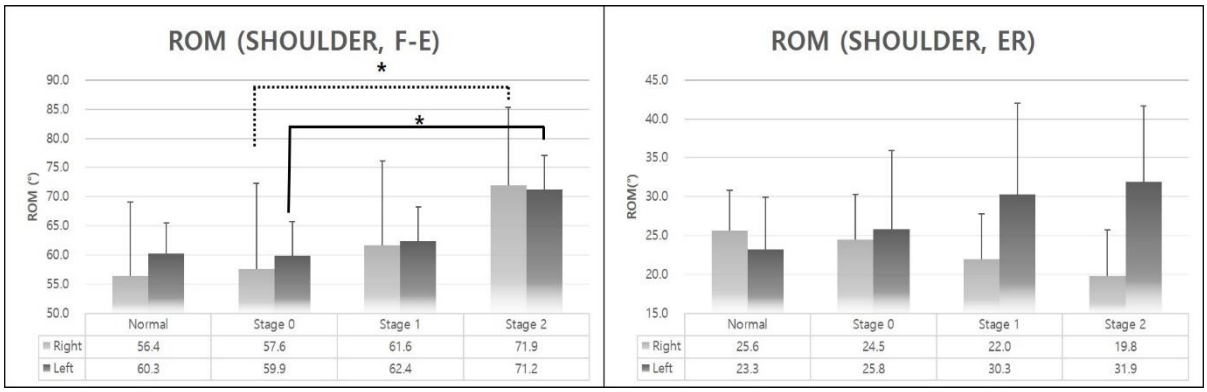

Graph 3. Shoulder ROM inflexion–extension and rotation.

2.2. Joint moment (in nanometer) during a gait

2.2.1. Elbow

The mean joint moment (in nanometer) of the dominant arm during a gait was 33.5±9.2 and 1.2±0.4 in the flexion–extension and pronation–supination, respectively. No significant difference exits between the normal swing (without brace) and stage 0 (with brace but free ROM; flexion–extension,

P=1.000; pronation–supination, *P*=1.000). In the dominant arm (right arm in all participants), the joint moment in flexion–extension was significantly increased in stages 1 and 2 compared with stage 0 (stage 0 vs 1, *P*=0.029; stage 0 vs 2, *P*<0.001). Moreover, no significant difference was noted in all comparison for ROM of pronation–supination between stages (stage 0 vs 1, *P*=0.943; stage 0 vs 2, *P*=1.000). In the nondominant arm (no brace, control group), the joint moment of the flexion–extension of stages 1 and 2 was significantly increased compared with stage 0 (stage 0 vs 1, *P*=0.001; stage 0 vs 2, *P*<0.001). Furthermore, no significant difference was noted in all comparison for ROM of pronation–supination between stages (stage 0 vs 1, *P*=0.743; stage 0 vs 2, *P*=0.970).

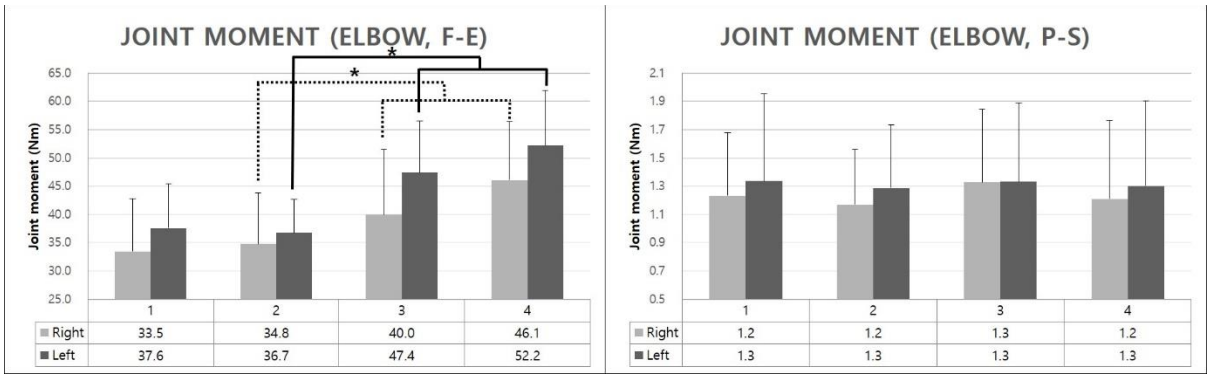

Graph 4. Joint moment of the elbow in flexion–extension and pronation–supination

2.2.2. Shoulder

The mean joint moment of the dominant arm during a gait was 91.3±22.6, 11.0±4.3, and 25.5±12.0 in flexion–extension, rotation, and abduction–adduction. No significant difference was noted between the normal swing (without brace) and stage 0 (flexion–extension, *P*=1.000; rotation, *P*=0.191; abduction, *P*=0.990). In the dominant arm, flexion–extension in stage 2 was significantly increased compared with stage 0 (stage 0 vs 1, *P*=0.569; stage 0 vs 2, *P*=0.005). Moreover, no significant difference exists in all comparison between stages in rotation (stage 0 vs 1, *P*=0.172; stage 0 vs 2, *P*=0.833) and abduction–adduction (stage 0 vs 1, *P* = 1.000; stage 0 vs 2, *P*=1.000). In the nondominant arm (no brace, control group), flexion–extension in stages 1 and 2 was significantly increased compared with stage 0 (stage 0 vs 1, *P*=0.039; stage 0 vs 2, *P*=0.015). Rotation in stages 1 and 2 were significantly increased compared with stage 0 (stage 0 vs 1, *P*<0.001; stage 0 vs 2,

P<0.001). No significant difference was noted in all comparison between stages in abduction–adduction (stage 0 vs 1, *P*=0.482; stage 0 vs 2, *P*=1.000).

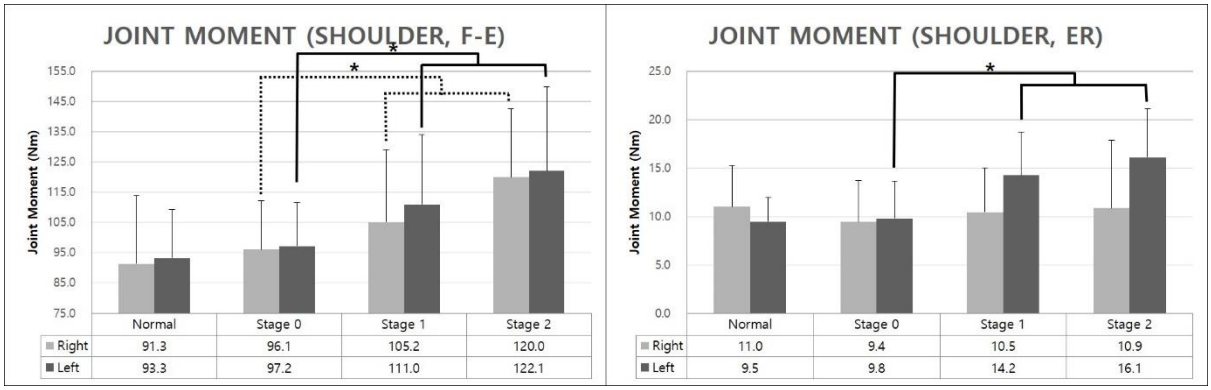

Graph 5. Joint moment of shoulder in flexion–extension and rotation

DISCUSSIONS

1. The elbow is a loadbearing joint

The elbow joint is not a weightbearing joint, and the joint line is perfectly parallel to the ground only in the neutral position. However, the motion of the shoulder would create a joint moment by gravitational force with the weight of the forearm in the elbow because the elbow is connected to the shoulder joint. Therefore, the elbow certainly takes weightbearing, not whole-body weight but forearm weight with the objects that may be carried in daily activity. The loading could be tremendously increased in sports activities (e.g., weightlifting, gymnastic, and any kind of racket sports). The knee and hip joint unlikely to take relatively unidirectional and consistent load created by body weight, and the elbow joint takes various weights according to the object to be held by hand or hung on the forearm and type of activity that may create various directional forces.

The muscles across the elbow (e.g., brachialis, biceps, and triceps) also create the joint moment in the elbow. The articular contact of the elbow in the biomechanical study was observed to be very minimum (almost zero) without muscle loading of brachialis, biceps, and triceps in the neutral position similar to the experimental setting of the current study. The gravity enables the distraction force for the elbow in the neutral position to be held only by collateral ligaments. However, once the

weights connecting each muscle (brachialis, biceps, and triceps) are placed, the joint moment was created against the gravity. In the results of a biomechanical study, the mean contact pressure in the neutral position with muscle loading (stage 0, resting) and during the forearm swing was 279.5±23.9 and 297.6±19.3 kPa, respectively. The swing motion was passively conducted by dropping the forearm, maintaining muscle loading. The mean contact pressure during swing motion showed no significant difference compared with the resting position (P=0.146). The muscle loading was translated to be enough to overcome the increased force for distraction created by gravity in the swing motion. The olecranon was crushed on the olecranon fossa at the endpoint of the swing motion. The crush also induces the increasing contact pressure of the coronoid in a moment and was presented as peak contact pressure. This crush motion probably happens in daily or sports activity, especially in racket sports or throwing. Thus, peak contact pressure was up to 513 kPa (mean, 420.7±54.3). However, it was not presented for the whole elbow joint because the Tekscan sensor for detecting contact pressure was not covered in the olecranon due to the methodology for the mounting sensor. Therefore, the peak contact pressure in the whole elbow joint was assumed to be higher than the measurement.

2. The stiffness increases the loading of the elbow

Loss of elbow motion due to arthritis is common and significantly compromises functional capabilities of the upper extremity. Continuous increased in articular contact pressure has been one of the initiators for the arthritic process. Arthritis is generally characterized by cartilage deterioration, subchondral bone sclerosis, and proliferation of new bone at the joint margin. Marginal osteophyte is the common pathology in the elbow joint, but it is also proliferated in the fossa that articulate with the coronoid and olecranon processes in flexion and extension. The articulation between the osteophyte in the fossa and marginal osteophyte in olecranon and coronoid processes mainly create the symptom of elbow arthritis including limited ROM and point pain. In the present biomechanical study, the pathologic condition of ROM in the extension due to the osteophyte in olecranon fossa was simulated by the K-wire block in olecranon fossa. The mean contact pressure in the *stiff model* (stage 2) was significantly increased compared with the *nonstiff model* (stage 0) in the resting and swing sessions

(*P*=0.001, resting; *P*=0.039, swing). Peak contact pressure in stage 2 was also highly increased compared with stage 0 (*P*=0.007). The results in the computational modeling of the stiff elbow also support the rejection of the first null hypothesis of the present study that (1) no difference exists in the articular contact pressure of the elbow by comparing between the *non-stiff* and *stiff models* in vivo study. For mimicking the elbow motion in stiffness, the elbow brace that allows the specific ROM was used. An extension block of 45° (stage 1) and 90° (stage 2) was set for different stiffness severity. In the flexion–extension axis, the joint moment of dominant elbow with stiffness was significantly increased compared with that without stiffness (stage 0 vs, *P*=0.019; stage 0 vs 2, *P*<0.001). This finding support the rejection of the third null hypothesis that (3) no difference of joint moment of the elbow and shoulder exists by comparing between *nonstiff* and *stiff models* in the arm swing of a gait. The stage 2 moment was significantly increased compared with that of stage 1 (stage 1 vs 2, *P*=0.026). This finding supports the rejection of the second and third null hypotheses that (2) the severity of stiffness would not affect the increase of the joint loading of the elbow.

3. Elbow stiffness increases the loading of shoulder joint in arm swing of a gait

Arm swing is a characteristic movement in human bipedal walking. The pendulum-like swing motion of the arms has been discovered to improve the stability and energy efficiency in human locomotion. Swinging arms create an angular momentum in the opposing direction of the lower limb rotation, reducing the total angular momentum of the body. The lower angular momentum of the body results in a decline on the ground reaction moment on the stance foot.[26] Therefore, the effective arm swing is required to be in symmetry with maintaining a certain trajectory in the angle of the elbow and shoulder joint. The stiffness of the elbow alters this symmetric trajectory by reducing the angle of the elbow. In the computational modeling of the arm swing in a gait, the ROM of flexion–extension in the shoulder joint with stiffness (stage 2) was significantly increased compared with that of stage 0 (stage 0 vs 2, *P*<0.001). The ipsilateral shoulder seems to compensate for the reduced angle of the elbow joint by increasing the angle of the shoulder in flexion–extension axis. The contralateral shoulder also seems to follow the ipsilateral shoulder motion to maintain the symmetric movement. Due to the increased shoulder motion and alteration of the moment, the arm with stiffness increases the joint

moment of both shoulder joints (stage 0 vs 2 in the dominant arm, P=0.005; stage 0 vs 1 in the nondominant arm, P=0.039; stage 0 vs 2, P=0.015). The finding supports the rejection of the third null hypothesis that (3) no difference exists in the joint moment of the elbow and shoulder by comparing between *nonstiff* and *stiff models* in the arm swing of a gait. Therefore, the finding of the current study conveys the meaningful message that the stiffness of the elbow joint increases the joint loading not only in the elbow joint but also in both shoulder joints by increasing the motion that may be the compensated motion against the shortened moment arm of the elbow stiffness. Even though the increase of the moment in a single gait is probably not meaningful, the accumulated joint loading may accelerate the arthritic process because the arm swing of the gait is continuously repeated in a lifespan.

4. Study strength and limitations

This is the first study to build up the stiff model of the elbow in a cadaveric study and computational musculoskeletal modeling using the markerless motion tracking sensor. With motion tracking-based computational modeling, the dynamic kinematics is now able to obtain and analyze the stiff elbow. The findings of the study could be a reference for further related studies.

This study has some limitations including the well-known limitations of any in vitro biomechanical study. The high mean age of the specimens could have affected the ligaments' tissue quality. However, all the specimens were evaluated for exclusion according to clinical signs of ligament insufficiency or macroscopic findings of ligament degeneration. The anterior capsule was excised, although it may not have a significant contribution to varus stability.[27, 28] The elbow was passively moved. Thus, knowing the effects of active muscle contraction and dynamic loading of the elbow is not possible. From a technical perspective, the Tekscan sensor has inherent limitations and the absolute values of contact pressure should be interpreted with caution. Although this study calibrated the sensors according to the manufacturer's recommendations, curved surface calibrations were not performed because it was not possible to calibrate the sensor used in this study on a curved surface that perfectly matched the contour of each elbow joint. The current study was not able to detect movement at the osteotomy site despite having performed a medial column osteotomy that could theoretically affect joint contact

pressures. It is unlikely that the osteotomy affected the results of the current study in any important way because all elbows were tested under the same condition.

CONCLUSIONS AND CLINICAL IMPLICATIONS

1. Conclusions

The elbow bears the load created by gravity and muscle contracture in the resting and dynamic arm swing movement. The stiffness of the elbow joint increases the loadbearing in the resting position and dynamic arm swing motion. The ipsilateral and contralateral shoulder joint seems to compensate for the decreased motion of the elbow by increasing the ROM of shoulder joints. Therefore, the moment of both shoulder joints was also increased.

2. Clinical implications

From a clinical perspective, the current study gives a strong reason that the stiffness of the elbow should be managed not only for pain relief and limited motion to minimize the inconvenience of daily activity but also to slow down the arthritic process by diminishing the joint loading.

References

1. Morrow MM, Hurd WJ, Kaufman KR, An KN. Upper-limb joint kinetics expression during wheelchair propulsion. *J Rehabil Res Dev.* 2009;46:939-944.

2. Chadwick EK, Blana D, van den Bogert AJ, Kirsch RF. A real-time, 3-D musculoskeletal model for dynamic simulation of arm movements. *IEEE Trans Biomed Eng.* 2009;56:941-948.

3. Magermans DJ, Chadwick EK, Veeger HE, van der Helm FC. Requirements for upper extremity motions during activities of daily living. *Clin Biomech (Bristol, Avon).* 2005;20:591-599.

4. Van Drongelen S, Van der Woude LH, Janssen TW, Angenot EL, Chadwick EK, Veeger DH. Mechanical load on the upper extremity during wheelchair activities. *Arch Phys Med Rehabil.* 2005;86:1214-1220.

5. van der Woude LH, Veeger HE, Dallmeijer AJ, Janssen TW, Rozendaal LA. Biomechanics and physiology in active manual wheelchair propulsion. *Med Eng Phys.* 2001;23:713-733.

6. Collins SH, Adamczyk PG, Kuo AD. Dynamic arm swinging in human walking. *Proc Biol Sci.* 2009;276:3679-3688.

7. Meyns P, Bruijn SM, Duysens J. The how and why of arm swing during human walking. *Gait Posture.* 2013;38:555-562.

8. Ballesteros ML, Buchthal F, Rosenfalck P. THE PATTERN OF MUSCULAR ACTIVITY DURING THE ARM SWING OF NATURAL WALKING. *Acta Physiol Scand.* 1965;63:296-310.

9. Koh SB, Park YM, Kim MJ, Kim WS. Influences of elbow, shoulder, trunk motion and temporospatial parameters on arm swing asymmetry of Parkinson's disease during walking. *Hum Mov Sci.* 2019;68:102527.

10. Lewek MD, Poole R, Johnson J, Halawa O, Huang X. Arm swing magnitude and asymmetry during gait in the early stages of Parkinson's disease. *Gait Posture.* 2010;31:256-260.

11. Morrey BF, Askew LJ, Chao EY. A biomechanical study of normal functional elbow motion. *J Bone Joint Surg Am.* 1981;63:872-877.

12. Søjbjerg JO. The stiff elbow. *Acta Orthop Scand.* 1996;67:626-631.

13. Masci G, Cazzato G, Milano G, et al. The stiff elbow: Current concepts. *Orthop Rev (Pavia).* 2020;12:8661.

14. Ramazanian T, Muller-Lebschi JA, Chuang MY, Vaichinger AM, Fitzsimmons JS, O'Driscoll SW. Effect of radiocapitellar Achilles disc arthroplasty on coronoid and capitellar contact pressures after radial head excision. *Journal of shoulder and elbow surgery.* 2018;27:1785-1791.

15. Bellato E, Fitzsimmons JS, Kim Y, et al. Articular Contact Area and Pressure in Posteromedial Rotatory Instability of the Elbow. *The Journal of bone and joint surgery. American volume.* 2018;100:e34.

16. Bellato E, Kim Y, Fitzsimmons JS, et al. Coronoid reconstruction using osteochondral grafts: a biomechanical study. *Journal of shoulder and elbow surgery.* 2017;26:1794-1802.

17. Bellato E, Kim Y, Fitzsimmons JS, et al. Role of the lateral collateral ligament in posteromedial rotatory instability of the elbow. *Journal of shoulder and elbow surgery.* 2017;26:1636-1643.

18. O'Driscoll SW. Classification and evaluation of recurrent instability of the elbow. *Clinical orthopaedics and related research.* 2000:34-43.

19. Drewniak EI, Crisco JJ, Spenciner DB, Fleming BC. Accuracy of circular contact area measurements with thin-film pressure sensors. *Journal of biomechanics.* 2007;40:2569-2572.

20. Brimacombe JM, Wilson DR, Hodgson AJ, Ho KC, Anglin C. Effect of calibration method on Tekscan sensor accuracy. *Journal of biomechanical engineering.* 2009;131:034503.

21. Niosi CA, Wilson DC, Zhu Q, Keynan O, Wilson DR, Oxland TR. The effect of dynamic posterior stabilization on facet joint contact forces: an in vitro investigation. *Spine.* 2008;33:19-26.

22. Bachman DR, Thaveepunsan S, Park S, Fitzsimmons JS, An KN, O'Driscoll SW. The effect of prosthetic radial head geometry on the distribution and magnitude of radiocapitellar joint contact pressures. *The Journal of hand surgery.* 2015;40:281-288.

23. Yeung LF, Yang Z, Cheng KC, Du D, Tong RK. Effects of camera viewing angles on tracking kinematic gait patterns using Azure Kinect, Kinect v2 and Orbbec Astra Pro v2. *Gait Posture.* 2021;87:19-26.

24. Oberg T, Karsznia A, Oberg K. Basic gait parameters: reference data for normal subjects, 10-79 years of age. *J Rehabil Res Dev.* 1993;30:210-223.

25. Reilly M, Kontson K. Computational musculoskeletal modeling of compensatory movements in the upper limb. *J Biomech.* 2020;108:109843.

26. Park J. Synthesis of natural arm swing motion in human bipedal walking. *J Biomech.* 2008;41:1417-1426.

27. Nielsen KK, Olsen BS. No stabilizing effect of the elbow joint capsule. A kinematic study. *Acta orthopaedica Scandinavica.* 1999;70:6-8.

28. Pollock JW, Brownhill J, Ferreira L, McDonald CP, Johnson J, King G. The effect of anteromedial facet fractures of the coronoid and lateral collateral ligament injury on elbow stability and kinematics. *The Journal of bone and joint surgery. American volume.* 2009;91:1448-1458.

국문 요약

배경 및 목적: 팔 흔들기 동작은 보행시 몸의 균형을 유지하고 앞으로 이동시키는 데 도움을 주는 중요한 역할을 한다. 본 연구는 주관절 구축이 보행시 견관절과 주관절에 미치는 생역학적인 영향을 연구하였다.

연구방법: 본 연구는 사체를 이용한 생역학실험과, 동작추적기술을 기반으로 하는 컴퓨터 시뮬레이션 기법을 이용한 연구로 구성된다. 사체를 이용한 생역학실험은 8 구의 신선동결사체를 이용하였다. 중력의 영향을 받고 주관절 주변부 근육의 힘을 구현할 수 있도록 자체 제작한 실험환경을 구현하였다. 관절 구축과 구축정도를 모사할 수 있는 주관절 구축모델을 3 단계로 (Stage 0- Stage 2) 만들었다. 근골격계 장애와 보행 장애가 없는 건강한 성인 남녀 15 명이 컴퓨터 시뮬레이션 실험에 참여하였다. 3 개의 심도측정센서 (Azure Kinect) 를 이용한 3 차원 동작 추적 시스템을 이용하여 관측하고자 하는 관절의 3 차원적 위치 정보를 얻을 수 있었다. 이를 바탕으로 관절의 부하 등의 생역학적 정보를 역추적하였다.

결과: 사체를 이용한 생역학실험에서, 구축이 없는 모델과 비교할 때 (stage 0) 60 도 구축 모델 (Stage 2) 에서 관절접촉압력이 유의하게 증가하였다. (mean contact pressure in the resting position, P<0.0001; mean contact pressure in the passive swing, P=0.039; peak contact pressure in the passive swing, P <0.007). 컴퓨터 시뮬레이션 모델에서는, 구축 모델이 (Stage 1 and 2) 구축이 없는 모델과 비교할 때, 대조군 주관절 (non-dominant elbow)의 관절범위가 (굴곡-신전) 유의하게 증가하였다. (stage 0 vs 1, P <0.001; stage 0 vs 2, P=0.008). 견관절의 관절범위 (굴곡-신전)는 Stage 2 에서부터 양팔 모두 유의하게 증가하였다. (stage 0 vs 2 in dominant, P<0.001; stage 0 vs stage 2 in nondominant, P<0.001). 구축 모델이 (Stage 1 and 2) 구축이 없는 모델과 비교할 때, 대조군 주관절 (non-dominant elbow)의 관절 모멘트(굴곡-신전) 또한 유의하게 증가하였다. (stage 0 vs 1, P=0.029; stage 0 vs 2, P<0.001 in dominant arm, stage 0 vs 1, P=0.001; stage 0 vs 2, P<0.001 in non-dominant arm) 견관절의 모멘트 (굴곡-신전)는 Stage 2 에서부터 양팔 모두 유의하게 증가하였다. (stage 0 vs 1, P=0.569; stage 0 vs 2, P=0.005 in dominant arm, stage 0 vs 1, P=0.039; stage 0 vs 2, P=0.015 in non-dominant arm).

결론: 주관절은 근육의 수축과 중력에 의해 관절 압력 부하를 받는다. 주관절의 구축은 이러한 관절 압력 부하를 증가시킨다. 구축된 동측 그리고 반대측 견관절은 이러한 주관절의 관절 구축으로 감소한 관절각도를 견관절의 관절범위 증가로 보상하려는 움직임을 보인다. 따라서 양측 어깨의 모멘트 또한 주관절 구축으로 인해 증가한다.